

Geological Society, London, Special Publications Online First

Automated forensic soil mineral analysis; testing the potential of lithotyping

Duncan Pirrie, Gavyn K. Rollinson, Matthew R. Power and Julia Webb

Geological Society, London, Special Publications, first published August 7, 2013; doi 10.1144/SP384.17

Email alerting service	click here to receive free e-mail alerts when new articles cite this article
Permission request	click here to seek permission to re-use all or part of this article
Subscribe	click here to subscribe to Geological Society, London, Special Publications or the Lyell Collection
How to cite	click here for further information about Online First and how to cite articles

Notes

Automated forensic soil mineral analysis; testing the potential of lithotyping

DUNCAN PIRRIE^{1*}, GAVYN K. ROLLINSON², MATTHEW R. POWER³ & JULIA WEBB⁴

¹*Helford Geoscience LLP, Menallack Farm, Treverva, Penryn, Cornwall TR10 9BP, UK*

²*Camborne School of Mines, College of Engineering, Mathematics & Physical Sciences, University of Exeter, Tremough Campus, Penryn TR10 9EZ, Cornwall, UK*

³*4669 West Lawn Drive, Burnaby, British Columbia, Canada V5C 3R2*

⁴*School of Natural and Social Sciences, University of Gloucestershire, Swindon Road, Cheltenham GL50 4AZ, UK*

**Corresponding author (e-mail: dpirrie@helfordgeoscience.co.uk)*

Abstract: In the investigation of serious crimes, soil can be, in some cases, a very valuable class of trace evidence. The complexity of soil is part of the reason why it is useful as trace evidence but is also an inherent problem, as there are many different parameters in a soil sample that could potentially be characterized. The inorganic components of soils are dominated by minerals, along with anthropogenic particulate grains; thus, the analysis of soil mineralogy as the main technique for inorganic forensic soil characterization is recommended. Typical methods that allow the bulk mineralogy to be determined, such as X-ray diffraction (XRD), do not allow the texture of the particles to be characterized. However, automated scanning electron microscopy (SEM) provides both modal mineralogy and also allows particle textures to be characterized. A recent advance in this technique has been the ability to report the modal mineralogy of a sample as 'lithotypes', which are defined on the basis of a combination of mineralogy and other parameters, such as grain size and mineral associations. Defined lithotype groups may include monomineralic grains but also, importantly, allow the automated quantification of rock types and other anthropogenic materials. Based on a simulated forensic scenario, the use of lithotyping is evaluated as an aid in the analysis of soil samples. This technique provides additional discrimination when comparing different soil samples.

The analysis of the composition of soils and sediments has become relatively widely used in forensic investigations in serious crime cases (e.g. Ruffell & McKinley 2008). The inherent variability of soils, at a variety of different scales, and the potential ease of transfer from scene to suspect or victim makes soil, in particular, a very useful class of trace evidence (Fitzpatrick *et al.* 2009). However, the complexity of soil also results in an issue as to what parameters of a soil sample should be characterized as part of a forensic investigation. Typically, the overall bulk characteristics of a soil can be measured, such as colour, grain size, pH or conductivity (e.g. Guedes *et al.* 2009, 2011). Alternatively, individual components within a soil may be selected for analysis. Most soils comprise both an organic and an inorganic component (e.g. Dawson & Hillier 2010). The organic component may include spores, pollen, macroscopic plant debris and micro-organisms, all of which can be forensically important (e.g. Brown 2006). The inorganic components of a soil will include naturally derived mineral grains from the underlying solid and drift geology,

along with anthropogenic particulate grains reflecting current or past land use at the specific sampling location. When considering the inorganic component, some workers have advocated the use of bulk chemical analysis of soil (although it should be noted that such an approach has also been strongly questioned: e.g. Bull *et al.* 2008), the analysis of the chemistry of specific mineral grains, the identification of the overall soil mineralogy (Pirrie *et al.* 2004) or the examination of the surface texture of discrete mineralogical components present within the soil (e.g. the examination of quartz grain shape: Bull & Morgan 2006).

At present, there is no standard approach to the geoforensic analysis of soil samples and, typically, individual practitioners will utilize the facilities available to them, or those that they have greatest experience of, although a common approach is to start with a more generalized examination of a sample which then becomes more focused. Pirrie *et al.* (2009) advocated the analysis of the overall mineralogy of soil samples as the most robust parameter to measure the inorganic components of a

soil. However, even with mineral analysis alone, there are different methods that might be used. Traditionally, mineral analysis in the geological sciences focused on the use of transmitted polarizing light microscopy, which with a trained operator allows both mineralogy and the sample texture to be quantified (see Bowen & Craven 2013 for a discussion on the value of transmitted light microscopy). Whilst still of considerable benefit in some cases, in a forensic context the sample size is commonly very small, and the material fine grained and, consequently, very difficult to identify using polarizing light microscopy. Another limitation with this method is that only translucent minerals can be identified; any opaque phases present will not be identified unless the sample is also examined using reflected light microscopy or scanning electron microscopy (SEM). There are two other relatively common methods to determine the overall bulk modal mineralogy: X-ray diffraction (XRD) and SEM with linked energy-dispersive spectrometers (EDS) (e.g. McVicar & Graves 1997; Ruffell & Wiltshire 2004). Both approaches have strengths and limitations. XRD identifies minerals on the basis of crystal structure. It is well suited to the analysis of clay minerals, although it should be noted that distinguishing between different clay mineral species requires the sample to be air dried, glycolated and heated in a stepwise approach. In addition, a recent validation of powder XRD found that minerals present in a known composite soil standard with a known abundance of up to about 9% were not identified (Eckardt *et al.* 2012). Bergliessen (2013) provides a thoughtful analysis of the strengths and limitations of XRD in a forensic context. As long as the XRD sample preparation and measurement parameters are clearly defined and adhered to, then this method does have some applications in forensic soil examination. Manual SEM-EDS analysis has also been widely used but it is difficult to generate quantitative datasets based on manual examination of a sample.

Automated SEM-EDS has the ability to characterize a large number of particles within a sample, based on the rapid acquisition of energy-dispersive spectra (Pirrie *et al.* 2004, 2009; Pirrie & Rollinson 2011). Mineral identification is based on the acquired chemical spectra, and limitations are that different minerals with the same, or very similar, chemistries cannot be distinguished from each other. If the modal mineralogy alone is reported, whether by XRD or automated SEM-EDS analysis, the texture of the sample is not known. For example, minerals may be present either as discrete particles composed of only a single mineral or they may be present within polymineralic grains, such as natural rock fragments or as fragments of anthropogenic materials, such as aggregates. Such textural

information can be very significant when testing the similarity, or otherwise, between different unknown samples. Previous work has shown how automated mineral analysis using QEMSCAN[®] SEM-EDS technology can characterize soil sample mineralogy (Pirrie *et al.* 2004, 2009).

In this paper, the potential forensic application of an additional function within the QEMSCAN[®] software that allows minerals to be grouped as 'lithotypes', which may be individual mineral grains, rock fragments or anthropogenic materials, is tested. The concept of lithotyping has recently been used in the oil and gas industry (Moscariello *et al.* 2010; Haberlah *et al.* 2012) to characterize the mineralogy and texture of well cuttings. The principle behind the technique is simple; individual particles are assigned to a compositional grouping based on expressions of their mineralogy along with other parameters, such as grain size, mineral associations, porosity and alteration. Thus, a coarse-grained rock fragment comprising quartz, alkali feldspar and plagioclase can be assigned as granite; a quartz sand with a calcite cement as a calcareous sandstone, and so on. Other particles within the sample may be monomineralic and can be assigned to a compositional grouping such as, for example, 'quartz grains'. In this way, the originally collected modal mineralogical data can be reassigned to lithotype groups, allowing the automated quantification of both mono- and polymineralic grains. This is effectively the same process as carried out during optical microscopy but is automated.

Experimental design, soil sampling and analysis

To test the potential value of the use of automated mineralogy to not only characterize soils based on the overall bulk mineralogy but also on the basis of lithotypes, a simple forensic scenario was replicated. Our simulated scenario was the surface disposal of a murder victim in an area of woodland in Cornwall, UK. The underlying bedrock geology comprises coarse-grained granites of the Carnmenellis Granite and minor superficial deposits (Fig. 1a) (Leveridge *et al.* 1990). The selected location had a discrete parking area, surfaced with aggregate, reached along a series of minor roads some 5 km from the nearest significant town, Falmouth (Fig. 1b). From the car parking area, a relatively flat track led into an area of light woodland with abundant understorey vegetation (Fig. 2a, b). This location was selected as it was consistent with known offender profiling with respect to the disposal of murder victims (e.g. distance from town, nature of roads, secluded parking location, deposition on the

AUTOMATED MINERAL ANALYSIS

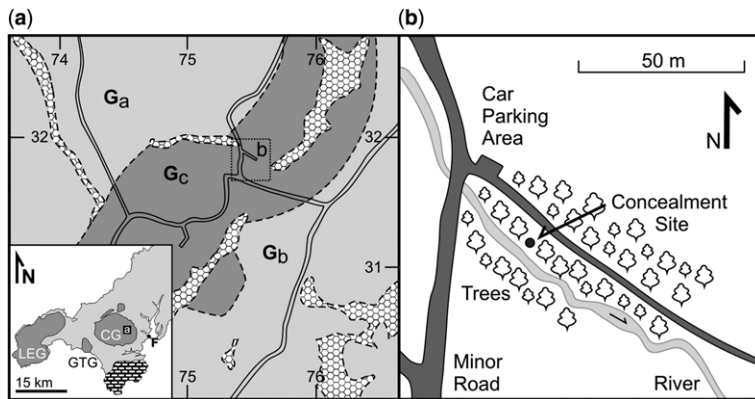


Fig. 1. Map showing the location of the study area (LEG, Lands End Granite; GTG, Godolphin-Tregonning Granite; CG, Carmenellis Granite; F, Falmouth). (a) The underlying bedrock geology is entirely underlain by the Carmenellis Granite and superficial deposits (adapted from Leveridge *et al.* 1990). G_a – coarse-grained granite abundant feldspar megacrysts > 15 mm; G_b – coarse-grained granite sparse feldspar megacrysts > 15 mm; G_c – coarse-grained granite abundant feldspar megacrysts < 15 mm. (b) Detailed map of the study area showing the car parking area, track and concealment site.

flat or down-hill and not more than 30 m from a car parking area). For the purpose of the simulation, two ‘offenders’ wearing previously used footwear but new denim jeans drove to the car parking area. Both individuals then entered the woodland along the track. One individual was carrying a 50-litre rucksack wrapped in plastic and filled with ballast to replicate carrying a small victim. The two ‘offenders’

made their way along the track (Fig. 2c), and then one individual branched off into the undergrowth and hid the object, having covered it with surface vegetation (Fig. 2d). The two offenders then left the scene and went back to their respective home locations. The following day, their footwear and jeans were both ‘seized’, with the items being sealed individually within paper evidence bags.



Fig. 2. Photographs illustrating the study area. (a) The car parking area adjacent to the area of woodland. (b) The track leading towards the concealment site. (c) Offender B carrying an object into the woodland. (d) The final concealed package covered by vegetation.

On the day after the concealment of the item, the scene was examined by other members of our research group, who had not been present during the concealment. A search of the area was carried out and the concealed item was located. The area between the track and the concealment site was heavily vegetated (Fig. 2d), and there were no exposed surface soils in amongst the vegetation. However, eight leaf litter samples were collected along the inferred offender approach path from the track to the concealment site. Fifteen soil samples were collected from the track (eight samples) and from the car parking area (seven samples). There were very common footwear tread marks along the track. The footwear tread of the offenders had not been described at the time of the scene visit; hence, it was not possible to specifically sample marks with a corresponding tread pattern. However, the footwear marks along the track were specifically targeted for sampling as they demonstrated that these areas had been recently contacted by footwear. Surface soil samples (to the depth of the observed tread marks) were collected from approximately 30 cm² areas by scraping the surface using a clean spatula, with the sample scrapped on to a piece of paper and then sealed within an evidence bag.

The surface of the car parking area was firmer than the surfaces along the track, although car tyre and diffuse footwear marks were observed. Consequently, samples collected in this area were collected in the same way as for the track but the sampling was of a shallower depth. The surface comprised soils, macroscopic plant debris and introduced geological materials, dominantly slates. There had been light rainfall both on the previous

day and on the day the samples were collected, so the soil samples collected were damp. Therefore, the samples were gently dried (<50 °C) within the laboratory as soon as possible.

The footwear and clothing were examined at the University of Gloucestershire. The two footwear items comprised (a) a pair of black shoes (Fig. 3a, b) and (b) a pair of white trainers (Fig. 3c, d). There was abundant soil present on the soles of both items of footwear, although soil was more abundant on the soles of the trainers (the footwear worn by the 'offender' carrying the object for disposal: Fig. 3a, c). The sides of the uppers of the trainers also had quite abundant soil present, whilst the uppers of the black shoes were generally visually clean of soil other than a small area of soil on the outer surface of the left shoe (Fig. 3b, d). The amount of soil present on the footwear exhibits was generally greater than that usually encountered during forensic casework. The soles and uppers of both the left and right item of both pairs of footwear were washed separately using a dilute detergent solution, centrifuged and the soil recovered. Two pairs of jeans were also examined. One pair was very clean with no obvious areas of soil staining. The other pair of jeans had several discrete mud spots at the rear and bottom of the right-hand leg. Both pairs of jeans were prepared in the same way. First, the lower part of each leg was cut off the jeans approximately 20 cm above the hem. Secondly, the area from just above the knee to the cut edge of the jeans was also removed. Thus, from each leg of each pair of jeans, two samples were recovered. Each separate piece of fabric was then washed using a dilute detergent solution and the resultant sample centrifuged. Separate sample



Fig. 3. Photographs showing footwear items (a) and (b) prior to the recovery of the soil trace evidence. (a) & (b) Uppers and sole of the right shoe from footwear item (a), a pair of black shoes. (c) & (d) Uppers and sole of the left shoe from footwear item (b), a pair of white patterned trainers.

AUTOMATED MINERAL ANALYSIS

aliquots were prepared from all of the footwear and clothing exhibits for (a) soil mineralogy and (b) palynology, although only the soil mineralogy is considered further in this paper. The soil samples collected from the access lane and car park area were subdivided with separate subsamples for palynology and mineralogy. The leaf litter samples were washed at the University of Gloucestershire, and the resultant debris was recovered and separate aliquots retained for palynology and mineralogy.

Mineralogical analysis

In total, 39 samples were prepared for mineral analysis. The samples were dried and then placed into clean 30 mm-diameter moulds. The samples were mixed with Epofix resin and then left in a pressure vessel overnight. The samples were then coded, and the moulds backfilled with resin and cured in an oven overnight. Samples were then cut and polished to a 1 μm finish and carbon-coated prior to analysis. Procedures for avoiding cross-contamination were followed throughout the preparation process. The samples were analysed at the University of Exeter, Cornwall Campus,

QEMSCAN[®] facility. They were measured using the QEMSCAN[®] particle mineral analysis (PMA) mode using a 6 μm beam stepping interval (see Pirrie *et al.* 2004). Typically, in excess of 6000 mineral grains were measured in each sample and the resultant raw dataset was processed using the iDiscover v.4.2 software package. The data were processed and reported in two different ways, (a) modal mineralogy and (b) lithotypes. Initially, the dataset was reported as individual mineral categories (modal mineralogy). In this way the data are processed such that any area analysed with the same, or very similar, chemistry is grouped either as a specific mineral species (e.g. quartz) or as a chemical grouping (e.g. CaAl silicate). The resultant modal mineralogical data are comparable with a traditional point-counting technique widely used in the measurement of, for example, sandstone petrography. When the data are reported purely as modal mineralogy, it is not documented as to whether the minerals are occurring as discrete grains of a single composition (e.g. a grain composed entirely of quartz or feldspar) or whether the grains are, in fact, polyminerallitic (e.g. either naturally occurring small rock fragments or as fragments

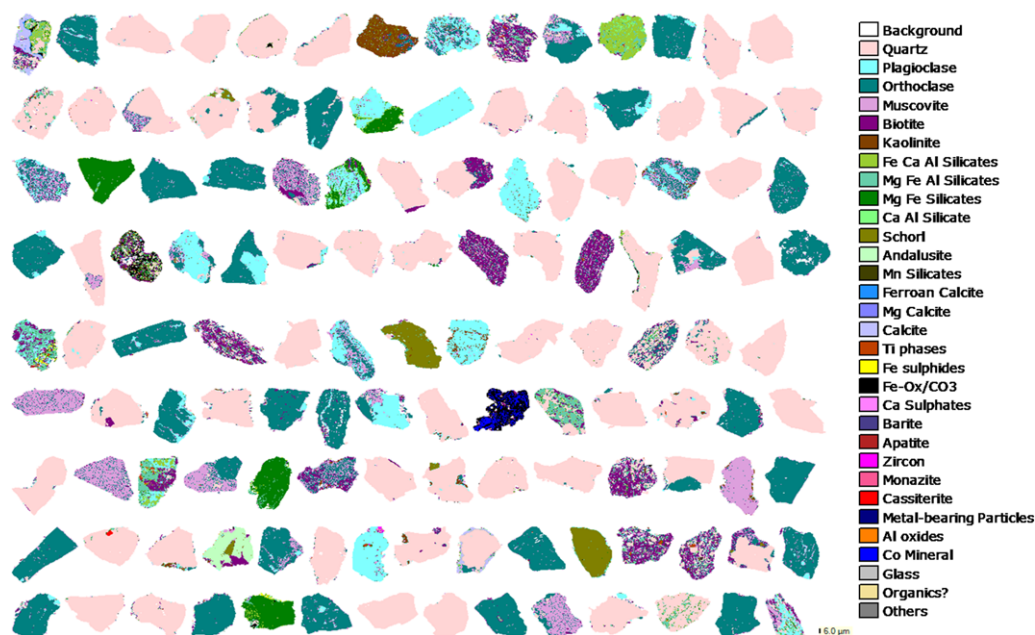


Fig. 4. Representative QEMSCAN[®] particle images arranged by area for one of the soil samples analysed. Note that the QEMSCAN[®] image shows that there are both particles composed of individual mineral grains (e.g. quartz, plagioclase, schorl) and composite particles composed of different mineral grains (i.e. rock fragments), such as grains composed of quartz and biotite with a well-defined fabric interpreted as metasedimentary rock fragments and coarse-grained quartz + orthoclase + plagioclase interpreted to be granite. Particles interpreted to be man-made also occur.

of aggregate). It is, however, possible to visualize this with the output of QEMSCAN[®] false-colour particle images (Fig. 4). It is also possible to quantify the mineral association data for the sample, which reflects the number of transitions between one mineral group and another between adjacent measured pixels (i.e. what is touching what).

The dataset was also reported as 'lithotypes'. A lithotype can either be a grain composed of a single mineral (e.g. a quartz lithotype) or polymineralic grains can be identified and assigned a rock name based on, for example, the observed mineralogy or grain size (e.g. a granite lithotype). Lithotyping effectively allows the dataset to be re-reported as discrete mineral grains, rock fragments or anthropogenic components. Lithotyping was first developed as an application tool for automated mineralogy in the analysis of oilfield drill cuttings (e.g. Moscariello *et al.* 2010; Haberlah *et al.* 2012) but can be equally applicable in any study where

the mineral particles present may be polyminerallic. The lithotype groupings are based on the standard geological definitions for rock types based on mineralogy, texture and grain or crystal size. As such, lithotyping is a means of generating automated quantitative petrographic data.

Results

The modal mineralogical data based on the QEMSCAN[®] analyses are presented first (a) as the overall sample modal mineralogy and then (b) grouped into lithotypes. The data from the concealment site are subdivided into three groupings: (a) soil from the car park area; (b) soil from the track; and (c) leaf litter washing samples collected along the offender approach path to the concealment site. The data from the two items of footwear are then considered. However, no more than 65 mineral grains were

Table 1. Modal mineralogical data for soil samples collected from the car parking area*

Sample name	OF/37	OF/38	OF/39	OF/40	OF/41	OF/42	OF/43
No. of analysis points	280 157	172 664	131 225	402 341	296 281	511 828	813 423
No. of particles	7447	7024	7345	7353	7710	7583	6492
Quartz	29.49	18.01	27.06	30.86	28.45	32.39	34.11
Plagioclase	15.80	12.30	11.86	12.87	13.77	9.94	10.15
Orthoclase	20.92	17.69	12.00	17.57	17.30	16.44	18.68
Muscovite	11.03	12.98	9.80	10.11	9.32	8.57	9.10
Biotite	8.54	17.75	16.70	14.55	14.03	15.84	16.77
Kaolinite	4.48	4.77	3.50	1.93	2.58	1.35	0.85
FeCaAl silicates	0.29	0.51	0.82	0.44	0.73	0.81	0.31
MgFeAl silicates	4.17	6.90	11.35	4.83	5.27	4.33	3.61
MgFe silicates	0.89	0.77	0.73	0.85	2.16	0.81	0.93
CaAl silicates	0.93	0.87	1.38	0.67	1.22	1.44	0.41
Schorl	1.35	4.81	1.11	2.52	1.37	2.54	1.70
Andalusite	0.07	0.11	0.14	0.04	0.06	0.03	0.08
Mn silicates	0.01	0.03	0.09	0.03	0.04	0.01	0.02
Ferroan calcite	0.12	0.17	0.16	0.21	0.47	0.55	0.17
Mg calcite	0.00	0.00	0.00	0.00	0.01	0.00	0.01
Calcite	0.28	0.13	0.49	0.71	1.58	2.95	1.76
Ti phases	0.43	0.36	0.62	0.36	0.34	0.38	0.29
Fe sulphides	0.01	0.05	0.04	0.01	0.07	0.09	0.04
FeO _x /CO ₃	0.65	1.35	1.56	1.03	0.64	0.80	0.62
Ca sulphates	0.03	0.01	0.05	0.02	0.03	0.03	0.01
Barite	0.00	0.01	0.01	0.00	0.00	0.00	0.00
Apatite	0.25	0.16	0.26	0.06	0.12	0.05	0.06
Zircon	0.06	0.10	0.09	0.05	0.09	0.06	0.03
Monazite	0.00	0.01	0.02	0.02	0.02	0.01	0.04
Cassiterite	0.01	0.01	0.00	0.04	0.01	0.14	0.05
Zn, Pb, Cu phases	0.00	0.01	0.00	0.01	0.01	0.01	0.00
Al oxides	0.11	0.08	0.06	0.11	0.08	0.08	0.08
Co mineral	0.00	0.00	0.00	0.00	0.00	0.00	0.00
Glass	0.02	0.02	0.03	0.05	0.19	0.30	0.09
Others	0.03	0.03	0.05	0.04	0.03	0.06	0.03

*Values shown as 0.00 may have the mineral present at an abundance of <0.01%.

AUTOMATED MINERAL ANALYSIS

identified in any of the washing samples recovered from the clothing samples. The low abundance of mineral grains on the clothing reflects the visual appearance of the clothing, which, other than several mud splash marks on one item, appeared clean, although Ruffell & Sandiford (2011) have suggested an improved method for soil recovery from clothing. The very low numbers of mineral particles located means that these samples are not considered further in this paper. Here, 'major' minerals are those forming >10% of the sample, 'minor' minerals are those between 1 and 10%, and 'trace' are <1%.

Modal mineralogy

The modal mineralogy of the soil samples collected from the car parking area is shown in Table 1. Between 6492 and 7710 individual mineral grains were characterized in the samples analysed. Major minerals present in these samples are quartz, plagioclase and orthoclase, along with major/minor

biotite, muscovite and MgFeAl silicates. Other minor phases present are kaolinite and schorl (tourmaline), along with minor/trace MgFe silicates, CaAl silicates, calcite and FeO_x/CO₃. Trace minerals present in some or all of the samples measured are FeCaAl silicates, andalusite, Mn silicates, ferroan calcite, Mg calcite, Ti phases, Fe sulphides, Ca sulphates, barite, apatite, zircon, monazite, cassiterite, Zn, Pb, Cu phases, Al oxides, glass and 'others'.

The modal mineralogical data for the track are presented in Table 2. Eight soil samples were collected along the track between the car parking area and the location where the offender approach path entered the woodland. Within these samples between 6399 and 8485 discrete mineral grains were identified per sample. The samples are dominated by major quartz, plagioclase and orthoclase, and minor muscovite, biotite and MgFeAl silicates, along with minor/trace kaolinite, schorl (tourmaline) and FeO_x/CO₃. A wide range of trace mineral phases also occur in some, or all, of the samples

Table 2. Modal mineralogical data for soil samples collected from the access track*

Sample name	OF/10	OF/30	OF/31	OF32	OF/33	OF/34	OF/35	OF/36
No. of analysis points	257 450	369 800	190 266	609 214	606 331	318 649	432 906	437 876
No. of particles	8485	6950	6399	6975	6897	6574	7108	6924
Quartz	37.67	39.63	38.16	41.88	42.56	40.01	38.60	32.79
Plagioclase	18.94	20.02	17.30	18.24	16.89	16.72	20.60	19.61
Orthoclase	14.04	21.87	17.55	24.90	22.05	22.98	21.73	23.81
Muscovite	9.42	8.46	10.31	7.59	8.85	7.68	9.22	10.48
Biotite	6.98	3.28	6.43	2.98	3.88	4.63	4.29	4.99
Kaolinite	2.08	1.37	1.71	0.77	0.79	1.29	1.57	2.53
FeCaAl silicates	0.21	0.10	0.16	0.14	0.09	0.11	0.08	0.15
MgFeAl silicates	6.10	1.66	2.81	0.79	1.34	2.11	1.27	1.35
MgFe silicates	0.65	0.20	0.29	0.40	0.22	0.49	0.45	0.56
CaAl silicates	0.53	0.30	0.85	0.24	0.28	0.32	0.37	0.52
Schorl	0.55	1.19	2.48	0.86	2.10	1.65	0.54	1.29
Andalusite	0.03	0.17	0.05	0.13	0.09	0.08	0.17	0.21
Mn silicates	0.08	0.01	0.04	0.00	0.01	0.02	0.01	0.01
Ferroan calcite	0.02	0.03	0.06	0.09	0.03	0.14	0.03	0.06
Mg calcite	0.00	0.00	0.00	0.00	0.00	0.00	0.00	0.00
Calcite	0.09	0.04	0.30	0.10	0.07	0.10	0.09	0.15
Ti phases	0.55	0.32	0.36	0.21	0.31	0.67	0.18	0.60
Fe sulphides	0.01	0.00	0.01	0.00	0.00	0.00	0.00	0.01
FeO _x /CO ₃	1.58	0.57	0.87	0.33	0.29	0.54	0.38	0.53
Ca sulphates	0.01	0.00	0.02	0.00	0.00	0.00	0.01	0.02
Barite	0.00	0.00	0.00	0.00	0.00	0.00	0.00	0.00
Apatite	0.20	0.44	0.07	0.23	0.05	0.19	0.23	0.19
Zircon	0.07	0.13	0.07	0.05	0.03	0.15	0.08	0.06
Monazite	0.11	0.03	0.02	0.01	0.03	0.04	0.01	0.03
Cassiterite	0.01	0.14	0.01	0.01	0.00	0.00	0.00	0.01
Zn, Pb, Cu phases	0.00	0.00	0.00	0.00	0.00	0.01	0.00	0.00
Al oxides	0.03	0.02	0.03	0.02	0.01	0.03	0.06	0.03
Co mineral	0.00	0.00	0.00	0.00	0.00	0.00	0.00	0.00
Glass	0.02	0.01	0.02	0.01	0.01	0.02	0.01	0.02
Others	0.01	0.01	0.02	0.01	0.00	0.01	0.01	0.02

*Values shown as 0.00 may have the mineral present at an abundance of <0.01%.

Table 3. Modal mineralogical data for the washing samples recovered from the leaf litter samples*

Sample name	OF/11	OF/12	OF/13	OF/14	OF/15	OF/16	OF/17	OF/18
No. of analysis points	14 500	4372	1068	3321	2992	2477	386	51 236
No. of particles	644	253	80	170	194	163	31	1619
Quartz	43.84	45.14	43.83	28.33	33.80	40.95	43.42	27.23
Plagioclase	14.71	14.80	5.71	6.94	13.60	13.60	0.77	16.20
Orthoclase	14.29	14.23	8.53	13.00	9.64	13.25	8.88	29.38
Muscovite	13.55	10.13	10.71	25.99	10.96	10.53	11.95	9.44
Biotite	6.60	2.91	10.62	3.22	6.00	4.55	1.29	5.18
Kaolinite	0.95	1.13	0.78	2.71	1.11	3.05	0.00	0.93
FeCaAl silicates	0.11	0.21	1.02	0.77	0.28	0.62	0.00	0.19
MgFeAl silicates	1.56	2.41	1.79	1.31	3.53	3.90	0.86	4.57
MgFe silicates	0.54	0.23	1.79	1.05	0.95	1.51	0.00	0.29
CaAl silicates	0.36	0.87	0.67	0.83	2.84	0.64	0.00	0.56
Schorl	0.36	0.64	0.84	0.00	0.12	1.17	0.00	2.01
Andalusite	0.18	0.00	0.00	0.00	0.00	0.00	0.00	0.02
Mn silicates	0.09	0.09	0.38	1.11	0.26	0.16	0.00	0.02
Ferroan calcite	0.16	0.03	0.00	0.03	0.26	0.00	0.00	0.82
Mg calcite	0.00	0.07	0.00	0.00	0.03	0.00	0.00	0.00
Calcite	0.68	2.91	0.00	1.09	4.85	0.81	30.55	0.16
Ti phases	0.24	1.10	0.27	0.13	0.39	0.89	0.00	0.68
Fe sulphides	0.00	0.00	0.00	0.00	0.00	0.00	0.00	0.01
FeO _x /CO ₃	1.41	2.22	13.07	6.72	7.45	3.84	0.81	1.05
Ca sulphates	0.01	0.02	0.00	0.02	0.00	0.00	0.00	0.75
Barite	0.00	0.00	0.00	0.00	0.00	0.00	0.00	0.00
Apatite	0.00	0.00	0.00	5.92	0.00	0.00	0.00	0.01
Zircon	0.11	0.04	0.00	0.10	0.34	0.14	0.90	0.05
Monazite	0.00	0.00	0.00	0.00	0.00	0.00	0.00	0.00
Cassiterite	0.00	0.00	0.00	0.00	0.00	0.00	0.00	0.00
Zn, Pb, Cu phases	0.00	0.00	0.00	0.00	0.12	0.00	0.00	0.00
Al oxides	0.01	0.00	0.00	0.09	0.43	0.16	0.00	0.27
Co mineral	0.00	0.00	0.00	0.00	0.00	0.00	0.00	0.00
Glass	0.21	0.02	0.00	0.03	0.10	0.12	0.00	0.00
Others	0.03	0.81	0.00	0.60	2.95	0.12	0.56	0.18

*Values shown as 0.00 may have the mineral present at an abundance of <0.01%.

including FeCaAl silicates, MgFe silicates, CaAl silicates, andalusite, Mn silicates, ferroan calcite, calcite, Ti phases, Fe sulphides, Ca sulphates, apatite, zircon, monazite, cassiterite, Zn, Pb, Cu phases, Al oxides and glass.

Eight samples of leaf litter were collected along the offender approach path from the track to the concealment site. Along this route there were no exposed soils. The leaf litter samples were washed to recover mineral grains and pollen. The number of mineral grains present in the samples analysed is very variable, ranging between 31 and 1619 discrete mineral grains. In most quantitative mineralogical studies a minimum of 300 grains is usually considered to be required for a data set to be considered to be statistically robust. In this case, only two samples had >300 mineral grains. It is, however, interesting to note that the modal mineralogical data for some of the samples with <300 grains are not dissimilar to the results for the samples with >300 grains. Although all of the data are

presented in Table 3, only those data for samples OF/11 and OF/18 are considered further. These two samples comprise major quartz, plagioclase and orthoclase, along with major/minor muscovite and minor biotite, MgFeAl silicates and FeO_x/CO₃. Schorl (tourmaline) and MgFe silicates are present as minor/trace phases in these two samples, along with trace kaolinite, FeCaAl silicates, CaAl silicates, andalusite, Mn silicates, ferroan calcite, calcite, Ti phases, Fe sulphides, Ca sulphates, apatite, zircon, Al oxides, glass and 'others'.

Soil samples were recovered from both the soles and uppers of both the left and right shoe of the two items of footwear. The modal mineralogical data for these eight samples are shown in Table 4. Between 5961 and 6522 mineral grains were identified in the four samples from the soles of the items of footwear, whilst between 1003 and 1810 were recovered from the washing samples recovered from the uppers of the two items of footwear, despite them

Table 4. Modal mineralogical data for the samples recovered from the two items of footwear*

Sample	Sole left shoe A	Uppers left shoe A	Sole right shoe A	Uppers right shoe A	Sole left trainer B	Uppers left trainer B	Sole right trainer B	Upper right trainer B
Sample name	OF/1/1	OF/1/2	OF/2/1	OF/2/2	OF/4/1	OF/4/2	OF5/1	OF/5/2
No. of analysis points	142 670	23 109	221 063	20 786	302 574	39 001	473 132	23 185
No. of particles	6522	1003	6215	1412	6278	1810	5961	1104
Quartz	34.36	21.28	35.15	26.96	36.67	33.45	34.54	27.45
Plagioclase	16.43	22.06	16.28	15.35	19.60	17.06	17.39	10.96
Orthoclase	12.26	12.47	20.18	10.04	20.11	15.03	23.44	8.45
Muscovite	13.06	13.75	13.55	16.15	10.24	13.45	9.27	9.38
Biotite	9.13	14.22	6.24	12.38	5.45	7.86	6.82	11.00
Kaolinite	2.27	2.78	2.18	2.81	2.68	2.93	1.97	1.90
FeCaAl silicates	0.33	0.64	0.20	0.43	0.19	0.24	0.18	0.16
MgFeAl silicates	4.75	3.26	2.10	5.36	1.29	2.61	1.81	2.63
MgFe silicates	0.59	1.90	0.56	2.37	0.60	0.85	0.82	0.93
CaAl silicates	1.51	1.74	0.68	1.61	0.60	0.88	0.30	0.68
Schorl	1.37	0.37	0.49	0.57	1.05	0.53	1.48	0.14
Andalusite	0.17	0.16	0.08	0.03	0.12	0.83	0.44	0.10
Mn silicates	0.01	0.01	0.02	0.00	0.01	0.07	0.00	0.00
Ferroan calcite	0.34	0.35	0.33	0.11	0.06	0.09	0.07	0.11
Mg calcite	0.00	0.07	0.00	0.00	0.00	0.22	0.00	0.30
Calcite	1.02	1.12	0.37	0.18	0.13	0.38	0.41	2.31
Ti phases	0.52	0.82	0.59	0.54	0.29	1.20	0.25	5.17
Fe sulphides	0.01	0.04	0.01	0.15	0.01	0.02	0.03	0.03
FeO _x /CO ₃	1.33	1.62	0.75	3.03	0.49	1.39	0.36	1.11
Ca sulphates	0.04	0.16	0.02	0.08	0.03	0.01	0.01	0.04
Barite	0.00	0.19	0.00	0.00	0.00	0.38	0.00	15.94
Apatite	0.13	0.02	0.08	0.31	0.16	0.19	0.18	0.24
Zircon	0.08	0.35	0.05	0.41	0.09	0.04	0.04	0.34
Monazite	0.01	0.00	0.01	0.00	0.02	0.00	0.02	0.03
Cassiterite	0.07	0.03	0.00	0.02	0.00	0.00	0.08	0.02
Zn, Pb, Cu phases	0.01	0.14	0.00	0.49	0.01	0.03	0.01	0.14
Al oxides	0.13	0.23	0.04	0.23	0.03	0.14	0.04	0.30
Co mineral	0.00	0.00	0.00	0.00	0.00	0.00	0.00	0.00
Glass	0.03	0.09	0.02	0.12	0.05	0.05	0.02	0.08
Others	0.04	0.13	0.02	0.26	0.01	0.04	0.01	0.06

*Values shown as 0.00 may have the mineral present at an abundance of <0.01%.

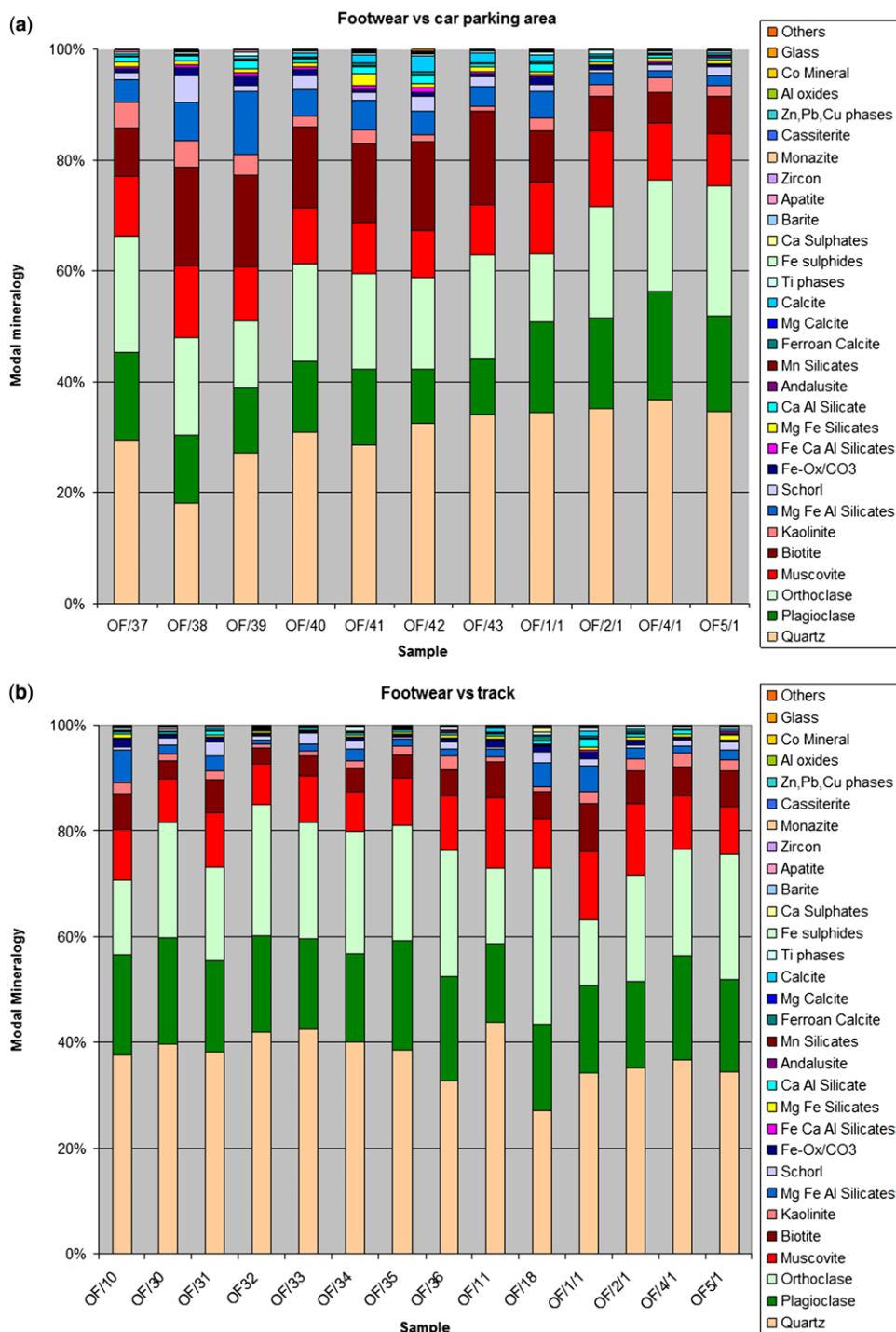


Fig. 5. Comparison of the overall modal mineralogy of: (a) the soil samples collected from the car parking area (OF/37, OF/38, OF/39, OF/40, OF/41, OF/42 and OF/43); and (b) soil samples from the access track (OF/10, OF/30, OF/31, OF/32, OF/33, OF/34, OF/35 and OF/36) and leaf litter (OF/11 and OF/18) with the mineralogy of the soil samples recovered from the soles of both items of footwear (OF/1/1, OF/2/1, OF/4/1 and OF/5/1).

AUTOMATED MINERAL ANALYSIS

Table 5. *Definitions for the lithotype groupings used in this study**

Lithotype grouping	Definition
Quartz grains	Area % of quartz >75%
Orthoclase grains	Area % of orthoclase >75%
Tourmaline grains	Area % of schorl >50%
Plagioclase grains	Area % of plagioclase >75%
Muscovite grains	Area % of muscovite >50%
Biotite grains	Area % of biotite >50%
Calcite grains	Area % of calcite >50%
Granite grains	Area % of feldspar >10% and size >40% or area % of feldspar >5% and area % of mica >5% and area % of feldspar + area % of mica >5% and area % of feldspar + area % of mica >75% or area % of quartz >5% and area % of mica >5% and area % of quartz + area % of mica >75% or area % of feldspar >75% or area % of quartz >5% and area % of feldspar >10% or area % of quartz >20% and area % of mica >10% or area % of quartz >50% or area % of kaolinite >10%
Metasediment	Area % of quartz >20% and area % of mica >10% or area % of quartz >50% or area % of kaolinite >10%
Chlorite	Area % of MgFeAl silicates >5% and area % of quartz >5% and area % of MgFeAl silicates + area % of quartz >50% or area % of MgFeAl silicates >75%
Kaolinite	Area % of kaolinite >50%
Tourmalinized granite	Area % of schorl >5% and area % of quartz >5% and area % of quartz and area % of schorl >50% or area % of schorl and area % of biotite >5% and area % of biotite and area % of schorl >50%
Cassiterite-bearing grains	Area % of cassiterite >0.5%
Al silicate grains	Area % of andalusite >50%
Mafic grains	Area % of MgFe silicate >50% or area % of plagioclase >5% and area % of MgFe silicate >5% and area % of plagioclase and area % of MgFe silicate 0.50%
Glass	Area % of glass >75%
Ti minerals	Area % of Ti phases >50%
Barium phases	Area % of barite >25%
Apatite	Area % of apatite >50%
Zircon/monazite	Area % of zircon >50% or area % of monazite >50%
Fe oxides and sulphides	Area % of FeO _x /CO ₃ >50 or area % of Fe sulphides >50%
Gypsum	Area % of Ca sulphate >50%
Calcareous sandstone	Area % of quartz >4% and area % of calcite >4%
CaAl silicate (glass/slag)	Area % of CaAl silicate >50% or area % of FeCaAl silicate >50%
Metal particles	Area % of Al oxide >50% or area % metal-bearing particles >50% or area % 5 Co mineral >50%
Aggregates of grains	Area % silicates >5%

*The expression of the definitions are as used in the iDiscover v 4.2 software.

appearing visually quite clean during examination. The samples are composed of major quartz, plagioclase and orthoclase, along with major/minor muscovite and biotite. Minor phases present in these samples are kaolinite and MgFeAl silicates, along with minor/trace MgFe silicates, CaAl silicates, schorl, calcite, Ti phases and FeO_x/CO₃. Trace phases present in all, or some, of these samples are FeCaAl silicates, andalusite, Mn silicates, ferroan calcite, Mg calcite, Fe sulphides, Cu sulphates, apatite, zircon, monazite, cassiterite, ZnPbCu phases, Al oxides, glass and 'others'. An anomaly that is discussed in greater detail below is that the soil sample recovered from the uppers of the right trainer is markedly different to the other footwear samples in that it also contained 15.94% of

spherical Ba–Sb particles. These particles are interpreted to be anthropogenic.

The modal mineralogical data for the soil samples collected from the soles of the two items of footwear are compared with the soil samples from (1) the car parking area (Fig. 5a) and (2) the track and the leaf litter samples (Fig. 5b). Based on the modal mineralogical data the soil samples from footwear item B (samples OF/4/1 and OF/5/1) are directly comparable with the modal mineralogical data for the soil samples collected along the access track, and would support a hypothesis that the soils present on footwear item B were derived through contact with the exposed soils present along the track. However, although the data for the right shoe from footwear item A (sample OF/2/1)

are comparable with the soil samples present from the access track, the data for the left shoe of footwear item A (sample OF/1/1) are more consistent with the data from the car parking area. Thus, the mineralogical data could be used to suggest that the individual wearing footwear item A did not enter the track leading to the concealment site. Where more than one individual is involved in a body deposition, it is not an unusual defence proposition that one or other of the individuals might have been present in an area but not directly involved in the victim deposition.

Thus, based on the modal mineralogical data alone, whilst the data are consistent with the hypothesis that footwear item B had contacted soils along the track leading to the body deposition site, the data are not entirely conclusive regarding whether or not footwear item A was only in contact with the soils in the car parking area, or whether the footwear also contacted exposed soils along the track.

Lithotype data

To test this hypothesis further the QEMSCAN[®] mineralogical data were reprocessed and exported

as lithotype groupings. The lithotype groupings used are shown in Table 5, and include: (a) grains that are composed of a single mineral type (e.g. plagioclase grains); (b) naturally occurring rock types (e.g. granite grains or tourmalinized granite); and (c) anthropogenic particle types (e.g. CaAl silicates (glass/slag)). The lithotype groupings are rigorously defined based on mineralogy and other parameters, and, once defined, all data can be output directly within these lithotype 'classes' and compared. Within a QEMSCAN[®] particle mineral analysis, false-colour maps of all particles are generated and these display the textures of the particles being measured in each sample. Effectively, the lithotype data enable the textural data displayed in the QEMSCAN[®] particle images to be quantified.

The lithotype data are presented in Tables 6–8, and are shown graphically in Figure 6a, b. In Figure 6a, b only the major/minor lithotype groups are plotted. As can be seen in Figure 6a, when the data for both items of footwear are compared with the data from the car parking area, although there are some similarities with some of the samples, the majority of the samples from the car parking area are distinctly different to the samples from

Table 6. *Lithotype data for the soil samples collected from the car parking area**

	OF/37	OF/38	OF/39	OF/40	OF/41	OF/42	OF/43
Quartz grains	25.66	13.53	18.48	27.57	25.47	28.21	31.38
Orthoclase grains	18.80	13.08	6.77	14.70	14.10	13.55	15.41
Tourmaline grains	0.71	3.88	0.22	1.91	0.80	2.05	1.20
Plagioclase grains	10.71	8.15	6.25	10.30	9.33	6.39	7.13
Muscovite grains	6.14	8.17	3.56	5.41	3.37	3.70	4.22
Biotite grains	4.21	12.78	6.31	11.77	9.32	13.33	18.13
Calcite grains	0.24	0.17	0.31	0.74	1.67	3.14	1.67
Granite grains	19.96	20.52	29.64	16.27	20.03	17.56	13.84
Metasediment	3.54	4.87	4.84	1.42	3.02	1.50	1.03
Chlorite	0.87	1.81	5.13	1.03	1.12	1.75	0.40
Kaolinite	2.69	3.13	2.13	1.14	1.53	0.81	0.52
Tourmalinized granite	0.42	0.52	0.86	1.47	0.48	0.94	1.36
Cassiterite-bearing grains	0.00	0.04	0.02	0.20	0.09	0.89	0.15
Al silicate grains	0.01	0.05	0.11	0.01	0.03	0.00	0.05
Mafic grains	1.55	0.70	0.45	1.09	2.12	0.28	0.92
Glass	0.00	0.00	0.00	0.00	0.08	0.00	0.00
Ti minerals	0.17	0.07	0.19	0.03	0.04	0.05	0.01
Barium phases	0.00	0.01	0.00	0.00	0.00	0.00	0.00
Apatite	0.21	0.12	0.21	0.02	0.10	0.01	0.00
Zircon/monazite	0.02	0.01	0.00	0.02	0.01	0.01	0.02
Fe oxides and sulphides	0.06	0.48	0.23	0.16	0.07	0.14	0.16
Gypsum	0.03	0.01	0.00	0.00	0.00	0.01	0.00
Calcareous sandstone	0.32	0.30	0.84	0.62	0.82	1.21	0.65
CaAl silicate (glass/slag?)	0.03	0.05	0.07	0.09	0.05	0.09	0.14
Metal particles	0.01	0.00	0.00	0.01	0.00	0.00	0.00
Aggregates of grains	0.12	0.34	1.06	0.47	0.40	0.22	0.10
Undifferentiated	3.52	7.22	12.34	3.57	5.93	4.18	1.49

*Values shown as 0.00 may have the lithotype present at an abundance of <0.01%.

AUTOMATED MINERAL ANALYSIS

the footwear. Thus, if one was testing the hypothesis that the soil on both footwear items was derived through contact with the exposed soils/surfaces in the car parking area, then the lithotype data for both sets of footwear would not support this hypothesis. If, however, the degree of similarity between the lithotype data for the footwear and the soil samples collected from the track leading towards the deposition site are considered (Fig. 6b), then the lithotype data would support a hypothesis that the soil on both items of footwear was consistent with contact between the footwear and the exposed soils along the track leading to the deposition site.

Discussion

Once a sample has been measured using automated mineralogy, the raw data can be output in a variety

of different formats. In this study, the data presented allow the overall modal mineralogy and the lithotype data to be compared, which, whilst based on the modal mineralogy, also identifies whether mineral particles are present as discrete mineral grains or as polymineralic grains (e.g. rock fragments). Thus, the lithotype data combine the mineralogical and textural data in exactly the same way as a geologist defines a rock type. Whilst there should be a broad correspondence between the two datasets, the lithotype data should allow the similarity or otherwise between two samples to be assessed more robustly than that based entirely on the modal mineralogical data. Indeed, this has been what has been done during forensic casework where, in addition to the overall modal mineralogy, the textural data contained within the QEMSCAN[®] particle images are also considered (see Fig. 4). The advantage of lithotyping is that this allows the mineralogical and textural data to be quantified.

Table 7. *Lithotype data for soil samples collected from the access track and also the leaf litter samples that comprised >300 grains**

	OF/10	OF/11	OF/18	OF/30	OF/31	OF/32	OF/33	OF/34	OF/35	OF/36
Quartz grains	30.43	42.20	22.54	35.90	34.24	40.52	41.56	38.18	36.28	30.24
Orthoclase grains	10.01	10.30	28.31	19.76	13.88	22.75	18.61	21.74	18.96	21.17
Tourmaline grains	0.34	0.12	2.39	0.83	2.33	0.79	1.84	1.34	0.34	0.87
Plagioclase grains	14.39	14.26	12.12	15.71	12.36	14.19	12.11	13.31	16.08	15.45
Muscovite grains	4.29	11.46	5.53	4.68	6.28	5.06	5.59	4.12	5.93	6.16
Biotite grains	1.86	5.40	2.37	1.22	3.16	1.74	2.37	2.68	2.74	3.08
Calcite grains	0.01	0.81	0.59	0.03	0.23	0.14	0.06	0.19	0.08	0.11
Granite grains	27.39	10.41	14.14	17.08	20.72	12.31	15.30	12.35	15.11	15.98
Metasediment	1.50	0.59	0.74	0.58	1.48	0.31	0.41	0.77	0.71	1.13
Chlorite	2.30	0.26	4.63	0.48	0.89	0.35	0.27	0.82	0.86	0.22
Kaolinite	1.24	0.75	0.36	0.60	0.63	0.17	0.27	0.63	0.84	1.91
Tourmalinized granite	0.17	0.10	0.09	0.44	0.08	0.06	0.03	0.60	0.25	0.20
Cassiterite-bearing grains	0.01	0.00	0.00	0.51	0.01	0.01	0.00	0.00	0.00	0.00
Al silicate grains	0.01	0.15	0.00	0.16	0.04	0.09	0.08	0.08	0.07	0.03
Mafic grains	0.65	0.65	0.20	0.16	0.24	0.48	0.23	0.55	0.69	0.89
Glass	0.00	0.18	0.00	0.00	0.00	0.00	0.00	0.00	0.00	0.00
Ti minerals	0.07	0.00	0.30	0.06	0.11	0.08	0.15	0.34	0.07	0.29
Barium phases	0.00	0.00	0.00	0.00	0.00	0.00	0.00	0.00	0.00	0.00
Apatite	0.18	0.00	0.00	0.37	0.06	0.19	0.04	0.16	0.19	0.13
Zircon/monazite	0.10	0.00	0.00	0.04	0.02	0.02	0.02	0.09	0.03	0.02
Fe oxides and sulphides	0.30	0.71	0.14	0.05	0.03	0.05	0.02	0.05	0.03	0.05
Gypsum	0.00	0.00	0.63	0.00	0.03	0.00	0.00	0.00	0.00	0.02
Calcareous sandstone	0.11	0.06	0.14	0.07	0.24	0.09	0.06	0.08	0.06	0.11
CaAl silicate (glass/slag?)	0.01	0.06	0.58	0.05	0.02	0.01	0.01	0.01	0.01	0.02
Metal particles	0.00	0.00	0.00	0.00	0.00	0.00	0.00	0.00	0.00	0.01
Aggregates of grains	0.37	0.00	0.25	0.02	0.08	0.02	0.07	0.02	0.01	0.06
Undifferentiated	4.26	1.51	3.95	1.20	2.85	0.56	0.89	1.87	0.65	1.86

*Values shown as 0.00 may have the lithotype present at an abundance of <0.01%.

Table 8. *Lithotype data for the samples recovered from the two items of footwear**

	OF/1/1	OF/1/2	OF/2/1	OF/2/2	OF/4/1	OF/4/2	OF/5/1	OF/5/2
Quartz grains	30.49	18.03	32.96	21.92	34.96	30.98	33.16	27.96
Orthoclase grains	9.40	9.10	16.98	4.71	17.74	10.55	22.41	5.82
Tourmaline grains	0.97	0.00	0.19	0.30	0.76	0.18	0.88	0.00
Plagioclase grains	12.28	15.88	12.52	10.12	17.68	10.42	13.58	9.07
Muscovite grains	7.91	8.01	10.31	9.84	6.44	10.06	6.38	5.94
Biotite grains	4.70	12.17	3.89	8.02	4.22	4.99	6.06	9.86
Calcite grains	1.19	1.08	0.57	0.21	0.14	0.52	0.43	2.98
Granite grains	19.65	17.83	15.37	25.44	11.87	20.51	10.77	13.64
Metasediment	2.77	3.63	1.47	3.47	1.35	1.96	0.81	1.08
Chlorite	1.41	1.05	0.45	0.96	0.24	1.39	0.59	1.12
Kaolinite	0.95	0.86	1.18	1.65	1.92	1.88	1.19	1.45
Tourmalinized granite	0.21	0.13	0.26	0.24	0.05	0.24	0.60	0.00
Cassiterite-bearing grains	0.00	0.20	0.00	0.22	0.00	0.00	0.31	0.20
Al silicate grains	0.06	0.12	0.04	0.00	0.07	0.74	0.47	0.00
Mafic grains	0.60	4.57	1.19	2.25	0.57	0.86	0.88	1.17
Glass	0.00	0.06	0.00	0.06	0.01	0.00	0.00	0.01
Ti Minerals	0.19	0.50	0.13	0.25	0.10	0.65	0.07	0.81
Barium phases	0.00	0.14	0.00	0.00	0.00	0.23	0.00	14.66
Apatite	0.10	0.00	0.05	0.28	0.11	0.18	0.07	0.23
Zircon/monazite	0.02	0.06	0.00	0.09	0.07	0.00	0.02	0.05
Fe oxides and sulphides	0.18	0.45	0.09	0.43	0.12	0.27	0.02	0.33
Gypsum	0.00	0.05	0.01	0.13	0.04	0.06	0.01	0.00
Calcareous sandstone	0.68	0.73	0.26	0.17	0.08	0.37	0.08	0.19
CaAl silicate (glass/slag?)	0.03	0.03	0.06	0.23	0.35	0.08	0.05	0.19
Metal particles	0.00	0.12	0.01	0.38	0.00	0.11	0.00	0.25
Aggregates of grains	0.38	0.35	0.01	0.61	0.01	0.00	0.00	0.00
Undifferentiated	5.85	4.85	2.00	8.03	1.11	2.78	1.18	2.97

*Values shown as 0.00 may have the lithotype present at an abundance of <0.01%.

In the case study presented in this paper, the modal mineralogical data alone supported the hypothesis that footwear item B had come into contact with the exposed soils along the track leading to the deposition site. However, the modal mineralogy data alone for footwear item A indicated that one of the pair of shoes had contacted the exposed soils, yet the data for the other item were ambiguous. In court, the data could be used to argue that the footwear could not be proven to have contacted the exposed soils, and that the data may have suggested that the footwear was only in contact with the exposed surfaces in the car park area. However, the lithotype data not only indicate that both items of footwear have contacted the exposed soils from the track leading to the deposition site but also indicate that the soils were not derived from contact with the exposed surfaces in the car park area. Thus, if this had been a real forensic case, then the lithotyping data would have been crucial in terms of testing alternative scenarios put forward as a defence.

Traditional mineralogical techniques such as polarizing light microscopy provide mineralogical data in a textural context. This is, however, difficult

to quantify, and, more significantly, from a forensic context, it is rare to have a sample of sufficient size to allow optical microscopy. Automated mineralogy with the ability to 'lithotype' the data set allows mineralogy and texture to be quantified. This is not possible based on other commonly used mineral analysis methods such as XRD. Similarly, whilst manual SEM of either sectioned and polished mineral grains, or the analysis of grain surface textures, can provide valuable data from a forensic context, it is difficult to rigorously quantify data from manual SEM.

Potential limitations to the application of lithotyping are that whilst data collection during automated mineralogy is operator independent, the processing of the data is not (Pirrie & Rollinson 2011). With lithotyping, the individual processing the raw data defines the mineralogical groupings used, as shown for this study in Table 5. Thus, the groups defined will, in part, be based on the experience and skill of the individual processing the data, and would need to be adapted on a case-by-case basis. From a forensic viewpoint, a dataset in which the lithotype groupings are defined too widely could potentially provide an inaccurate

AUTOMATED MINERAL ANALYSIS

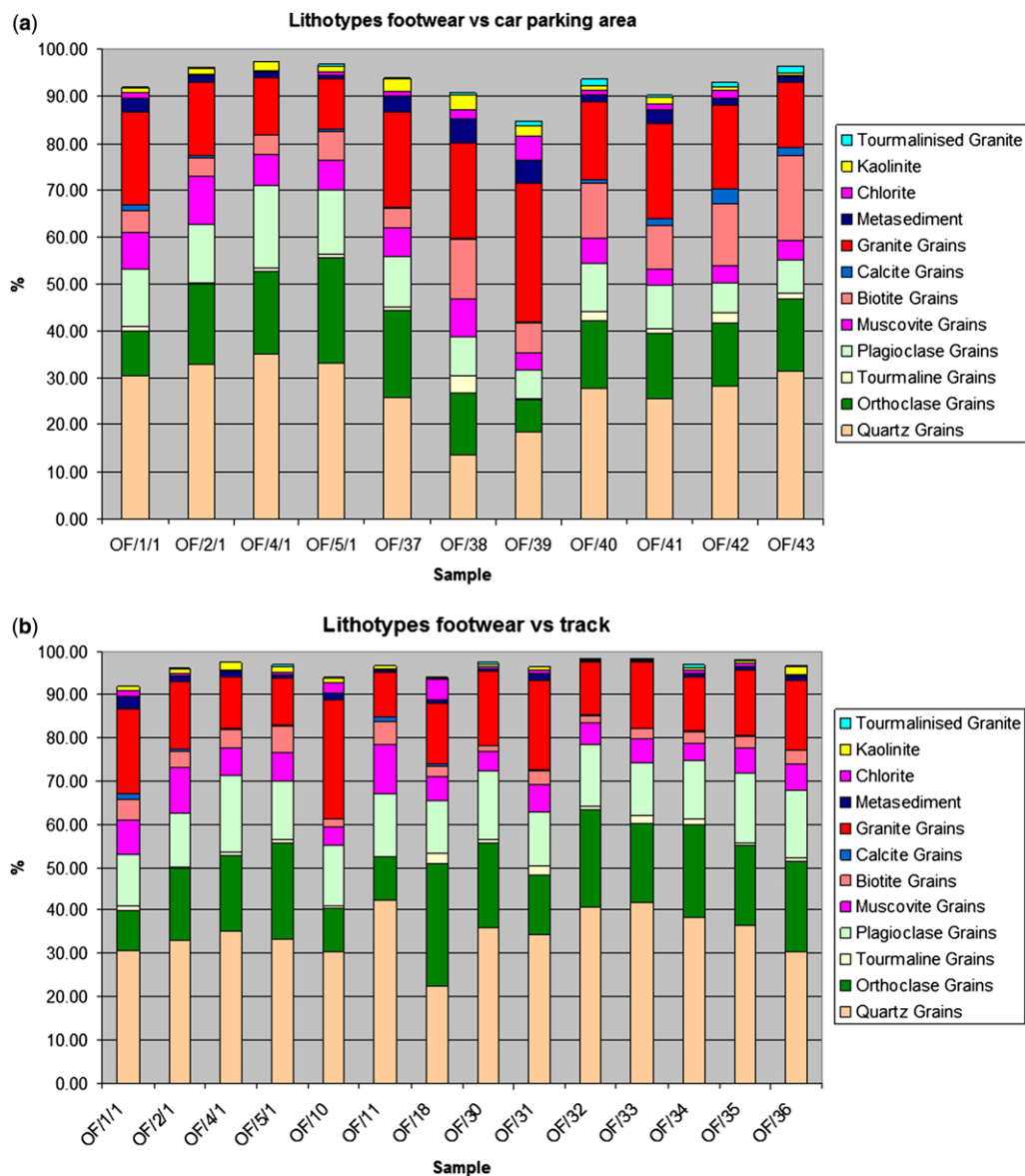


Fig. 6. Comparison of the relative abundance of the major/minor lithotypes present in: (a) the soil samples collected from the car parking area (OF/37, OF/38, OF/39, OF/40, OF/41, OF/42 and OF/43); and (b) soil samples from the access track (OF/10, OF/30, OF/31, OF/32, OF/33, OF/34, OF/35 and OF/36) and leaf litter (OF/11 and OF/18) with the soil samples recovered from the soles of both items of footwear (OF/1/1, OF/2/1, OF/4/1 and OF/5/1).

degree of similarity between different samples. In contrast, a lithotyping study in which the groupings were very tightly defined would provide a robust test of the level of similarity between different samples. If lithotyping were to become widely adopted in criminal soil forensics, clearly defined protocols for the lithotype groupings could be

defined and adhered to. However, no two studies are identical as a result of the wide variability of soils and, as such, the lithotype groupings would still have to be adapted on a case-by-case basis.

Finally, an additional advantage of an automated mineralogy approach to soil forensics, whether with the reporting of the results as overall modal



Fig. 7. QEMSCAN[®] particle images for a spherical Ba–Sb phase present on the uppers of footwear item (b). The source of these particles is unknown.

mineralogy or as lithotypes, is that all particle types present are characterized. In this study, a surprising result was that in the sample recovered by washing the uppers of the right white trainer (footwear item B), 15.94% of the particles present reported to the mineral category 'barite'. However, these particles, which are characteristically spherical in shape (Fig. 7), are a Ba–Sb phase and are interpreted as anthropogenic particulates. Similar particle types were not recovered in the soil samples from the car parking area, access lane or concealment site, although two spherical Ba–Sb particles were present in the washing sample from the uppers of the left white trainer (footwear item B). Whilst Sb–Ba particles are considered to be consistent with particles formed during the discharge of a firearm (ASTM 2010), spherical particles of Ba–Sb are known from, for example, the use of fireworks (Grima *et al.* 2012) and are also known to occur from motor vehicle disk brakes, although in this case the particles are not typically spherical in shape (Garofano *et al.* 1999). The source of the Ba–Sb particles in this study is not known. Although the shoes were pre-worn prior to this field trial, the owner denies: (a) discharging a firearm whilst wearing the footwear or being close to a firearm when being discharged; (b) being in close proximity to fireworks whilst wearing the footwear; or (c) having come into contact with motor vehicle brake shoes. It is, however, interesting to note that the area used for the concealment of the item is occasionally used by individuals for shooting, and also a sculptor who works using metal frequently stores items in, and around, the car parking area. It should, however, be noted that no spherical Ba–Sb particles were recovered in any of the soil samples analysed and there were no Ba–Sb particles present on the other item of footwear.

Conclusions

One of the key reasons why soil is an important and useful class of trace evidence is because of its

complexity and variability (e.g. Fitzpatrick *et al.* 2009). Its complexity also brings with it an inherent issue in that, whilst ideally in a forensic context one would wish to examine several different parameters within the soil, there is no standard protocol as to what aspects of a soil should be examined. Whilst numerous papers have advocated the use of grain size, colour and bulk chemistry as a means of discriminating between different soils, all of these attributes have inherent problems when viewed from a forensic context. For instance, it is widely recognized that there may be differential transfer and retention of different particle sizes on, for example, different types of clothing, such that a direct comparison between the grain size of soil on clothing v. the grain size of a soil at a scene may provide a false negative response (although see Morgan & Bull 2007). Colour can at best be used to exclude the possibility of a similar origin of two questioned soils of different colours but a similarity in colour does not provide sufficient evidence to indicate an association between two soils. Bulk chemistry is not only destructive but may also provide either false positive or false negative interpretations. Characterizing the mineralogy of soils is the most important way in our opinion to discriminate between samples based on the inorganic components present. If through automated mineralogy this can be combined with particle texture and mineralogical associations, then it allows even the typically very small samples encountered in forensic casework to be fully characterized geologically. This allows a greater degree of precision when evaluating whether or not an unknown sample could have been derived through contact with soils at a known location. However, lithotyping is potentially also very significant as a means of providing critical provenance and geolocation data where a soil sample is being examined to try to identify the potential location(s) from where that soil may have been derived. The data in this study are consistent with the dominant soils in the area being derived from a granitic bedrock geology. In particular, the underlying geology is composed of the coarse-grained granite comprising alkali

AUTOMATED MINERAL ANALYSIS

feldspar, plagioclase, quartz, biotite white mica and tourmaline (Leveridge *et al.* 1990). The reason why the soil samples present in the car parking area were distinctive when compared with the track is because this surface had been dressed with metasedimentary rock fragments, predominantly slates, as a hard-core, and this is reflected in the lithotype data set. It is this introduced material that made the car parking area distinctive from the track and the concealment site.

We are grateful for the ongoing support and interest in our research from Dr A. Butcher (FEI Company), P. Frost and G. Rollinson (CSM) both kindly donated clothing and footwear for analysis, and were willing volunteers during the clandestine disposal of the object in the woodland (without being caught). B. Snook is thanked for assistance in preparing the figures and H. Campbell commented on early drafts of the manuscript. We are grateful for the comments of the referees.

References

- ASTM 2010. *E-1588-10. Standard Guide for Gunshot Residue Analysis by Scanning Electron Microscopy/ Energy Dispersive X-ray Spectrometry*. ASTM International, West Conshohocken, PA.
- BERGLIEN, E. T. 2013. X-ray diffraction and field portable X-ray fluorescence analysis and screening of soils: project design. In: PIRRIE, D., RUFFELL, A. & DAWSON, L. A. (eds) *Environmental and Criminal Geoforesics*. Geological Society, London, Special Publications, **384**, first published online July 16, 2013, <http://dx.doi.org/10.1144/SP384.14>
- BOWEN, A. M. & CAVEN, E. A. 2013. Forensic provenance investigations of soil and sediment samples. In: PIRRIE, D., RUFFELL, A. & DAWSON, L. A. (eds) *Environmental and Criminal Geoforesics*. Geological Society, London, Special Publications, **384**, first published online May 16, 2013, <http://dx.doi.org/10.1144/SP384.4>
- BROWN, A. G. 2006. The use of forensic botany and geology in war crimes investigations in NE Bosnia. *Forensic Science International*, **163**, 204–210.
- BULL, P. A. & MORGAN, R. M. 2006. Sediment fingerprints: a forensic technique using quartz sand grains. *Science and Justice*, **46**, 64–81.
- BULL, P. A., MORGAN, R. M. & FREUDIGER-BONZON, J. 2008. A critique of the present use of some geochemical techniques in geoforensic analysis. *Forensic Science International*, **178**, e35–e40.
- DAWSON, L. A. & HILLIER, S. 2010. Measurement of soil characteristics for forensic applications. *Surface and Interface Analysis*, **42**, 363–377.
- ECKARDT, R., KRUPICKA, E. & HOFMEISTER, W. 2012. Validation of powder X-ray diffraction following EN ISO/IEC 17025. *Journal of Forensic Science*, **57**, 722–737.
- FITZPATRICK, R. W., RAVEN, M. D. & FORRESTER, S. T. 2009. A systematic approach to soil forensics: criminal case studies involving transference from crime scene to forensic evidence. In: RITZ, K., DAWSON, L. & MILLER, D. (eds) *Criminal and Environmental Soil Forensics*. Springer, Heidelberg, 105–127.
- GAROFANO, L., CAPRA, M., FERRARI, F., BIZZARO, G. P., DI TULLIO, D., DELL'OLIO, M. & GHITTI, A. 1999. Gunshot residue further studies on particles of environmental and occupational origin. *Forensic Science International*, **103**, 1–21.
- GRIMA, M., BUTLER, M., HANSON, R. & MOHAMEDEN, A. 2012. Firework displays as sources of particles similar to gunshot residue. *Science and Justice*, **52**, 49–57.
- GUEDES, A., RIBEIRO, H., VALENTIM, B. & NORONHA, F. 2009. Quantitative colour analysis of beach and dune sediments for forensic applications: a Portuguese example. *Forensic Science International*, **190**, 42–51.
- GUEDES, A., RIBEIRO, H., VALENTIM, B., RODRIGUES, A., SANT'OVAIA, H., ABREU, I. & NORONHA, F. 2011. Characterisation of soils from the Algarve region (Portugal): a multidisciplinary approach for forensic applications. *Science and Justice*, **51**, 77–82.
- HABERLAH, D., BOTHA, P. W. S. K., DOBRZINSKI, N., BUTCHER, A. R. & KALDI, J. G. 2012. Petrological reconstruction of the subsurface based on PDC drill cuttings: an advanced rock typing approach. In: BROEKMANS, M. A. T. M. (ed.) *Proceedings of the 10th International Congress for Applied Mineralogy (ICAM)*. Springer, Heidelberg, 275–283.
- LEVERIDGE, B. E., HOLDER, M. T. & GOODE, A. J. J. 1990. *Geology of the Country Around Falmouth*. Geological Memoirs & Sheet Explanations (England & Wales), **352**. British Geological Survey, Keyworth, Nottingham.
- MCVICAR, M. J. & GRAVES, W. J. 1997. The forensic comparison of soils by automated scanning electron microscopy. *Journal of the Canadian Society of Forensic Scientists*, **30**, 241–261.
- MORGAN, R. M. & BULL, P. A. 2007. The use of grain size distribution analysis of sediments and soils in forensic enquiry. *Science and Justice*, **47**, 125–135.
- MOSCARIELLO, A., BURNS, S., WALKER, D., POWER, M. R., KITSON, W. S. & SLIWINSKI, J. 2010. Sequence stratigraphy and reservoir characterisation of barren fluvial sequences using rock-typing analyses of core and cuttings. *AAPG GEO 2010 Middle East Geoscience Conference & Exhibition. Innovative Geoscience Solutions – Meeting Hydrocarbon Demand in Changing Times*, 7–10 March, Manama, Bahrain. http://www.searchanddiscovery.com/abstracts/html/2010/geo_bahrain/abstracts/Moscariello.html
- PIRRIE, D. & ROLLINSON, G. K. 2011. Unlocking the applications of automated mineral analysis. *Geology Today*, **27**, 226–235.
- PIRRIE, D., BUTCHER, A. R., POWER, M. R., GOTTLIEB, P. & MILLER, G. L. 2004. Rapid quantitative mineral and phase analysis using automated scanning electron microscopy (QemSCAN): potential applications in forensic geoscience. In: PYE, K. & CROFT, D. J. (eds) *Forensic Geoscience: Principles, Techniques and Applications*. Geological Society, London, Special Publications, **232**, 123–136.
- PIRRIE, D., POWER, M. R., ROLLINSON, G. K., WILTSHIRE, P. E. J., NEWBERRY, J. & CAMPBELL, H. E. 2009. Automated SEM-EDS (QEMSCAN®) mineral analysis in forensic soil investigations: testing instrumental

D. PIRRIE *ET AL.*

- reproducibility. In: RITZ, K., DAWSON, L. & MILLER, D. (eds) *Criminal and Environmental Soil Forensics*. Springer, Heidelberg, 411–430.
- RUFFELL, A. & WILTSHIRE, P. 2004. Conjunctive use of quantitative and qualitative X-ray diffraction analysis of soils and rocks for forensic analysis. *Forensic Science International*, **145**, 13–23.
- RUFFELL, A. & MCKINLEY, J. 2008. *Geoforensics*. Wiley, New York.
- RUFFELL, A. & SANDIFORD, A. 2011. Maximising trace soil evidence: An improved recovery method developed during investigation of a \$26 million bank robbery. *Forensic Science International*, **209**, e1–e7.